

Molecular Characterization of the Multiple Interactions of SpsD, a Surface Protein from *Staphylococcus pseudintermedius*, with Host Extracellular Matrix Proteins

Giampiero Pietrocola¹, Joan A. Geoghegan², Simonetta Rindi¹, Antonella Di Poto¹, Antonino Missineo¹, Valerio Consalvi³, Timothy J. Foster², Pietro Speziale^{1*}

1 Department of Molecular Medicine, Institute of Biochemistry, Pavia, Italy, **2** Department Microbiology, Moyné Institute of Preventive Medicine, Trinity College, Dublin, Ireland, **3** Department of Biochemical Sciences "A. Rossi Fanelli", University of Rome "La Sapienza", Roma, Italy

Abstract

Staphylococcus pseudintermedius, a commensal and pathogen of dogs and occasionally of humans, expresses surface proteins potentially involved in host colonization and pathogenesis. Here, we describe the cloning and characterization of SpsD, a surface protein of *S. pseudintermedius* reported as interacting with extracellular matrix proteins and corneocytes. A ligand screen and Western immunoblotting revealed that the N-terminal A domain of SpsD bound fibrinogen, fibronectin, elastin and cytokeratin 10. SpsD also interfered with thrombin-induced fibrinogen coagulation and blocked ADP-induced platelet aggregation. The binding site for SpsD was mapped to residues 395–411 in the fibrinogen γ -chain, while binding sites in fibronectin were localized to the N- and C-terminal regions. SpsD also bound to glycine- and serine-rich omega loops within the C-terminal tail region of cytokeratin 10. Ligand binding studies using SpsD variants lacking the C-terminal segment or containing an amino-acid substitution in the putative ligand binding site provided insights into interaction mechanism of SpsD with the different ligands. Together these data demonstrate the multi-ligand binding properties of SpsD and illustrate some interesting differences in the variety of ligands bound by SpsD and related proteins from *S. aureus*.

Citation: Pietrocola G, Geoghegan JA, Rindi S, Di Poto A, Missineo A, et al. (2013) Molecular Characterization of the Multiple Interactions of SpsD, a Surface Protein from *Staphylococcus pseudintermedius*, with Host Extracellular Matrix Proteins. PLoS ONE 8(6): e66901. doi:10.1371/journal.pone.0066901

Editor: Brian Stevenson, University of Kentucky College of Medicine, United States of America

Received: March 7, 2013; **Accepted:** May 12, 2013; **Published:** June 21, 2013

Copyright: © 2013 Pietrocola et al. This is an open-access article distributed under the terms of the Creative Commons Attribution License, which permits unrestricted use, distribution, and reproduction in any medium, provided the original author and source are credited.

Funding: The support by Fondazione CARIPLO 'Vaccines 2009-3546' to P. Speziale is acknowledged. TJF acknowledges the support of Science Foundation Ireland [grant number 08/IN.1/B1845]. The funders had no role in study design, data collection and analysis, decision to publish, or preparation of the manuscript.

Competing Interests: The authors have declared that no competing interests exist.

* E-mail: pspeziale@unipv.it

Introduction

Staphylococcus pseudintermedius is a commensal and opportunistic pathogen of companion animals, especially dogs [1,2], mainly causing skin infections such as pyoderma as well as surgical wound infections, urinary tract infections and otitis externa. Cases of infections in humans have occasionally been reported [3–6]. Methicillin-resistant *S. pseudintermedius* occurs widely [7,8]. The complete genome sequences of two isolates of *S. pseudintermedius* are available [9,10]. The strains are predicted to encode many putative virulence factors including toxins, extracellular enzymes such as lipases and proteases and surface proteins designated *S. pseudintermedius* surface proteins A–R (SpsA–R) [11] some of which are known to promote adhesion of the bacterium to desquamated skin epithelial cells (corneocytes) [12–14] and to components of the extracellular matrix [11,15].

One such surface protein that is likely to be important in skin colonization and virulence is SpsD. The presence of SpsD on the bacterial cell surface promotes adhesion to fibrinogen (Fbg), fibronectin (Fn) and cytokeratin 10 (K10). Immunoglobulin G specific for SpsD occurs in dogs with pyoderma indicating that the protein is expressed during infection [11]. SpsD has many features that are typical of staphylococcal surface proteins called microbial

surface components recognizing adhesive matrix molecules (MSCRAMMs) that are related to clumping factors (Clf) and fibronectin binding proteins (FnBPs) of *S. aureus* [11].

The primary translation product of SpsD has an N-terminal secretory signal sequence and a C-terminal sorting signal comprising an LPXTG motif for sortase A-mediated linkage to peptidoglycan, a hydrophobic membrane-spanning domain and positively charged residues. The N-terminus of the mature protein comprises an A domain, part of which has sequence similarity to the A domains of ClfA and FnBPs (Figure 1).

The A domains of FnBPA and FnBPB show significant sequence similarity to ClfA and are predicted to fold into three independent subdomains, N1, N2 and N3. The ligand binding sites within ClfA, FnBPA and FnBPB are confined to the N2 and N3 subdomains and they each bind to the C-terminus of the γ -chain of Fbg most likely by the same "dock, lock and latch" mechanism [16–18]. X-ray crystal structure analysis of ClfA revealed that the apo form of the protein adopts an open conformation with an exposed hydrophobic trench located between separately folded N2 and N3 subdomains. Binding of the Fbg γ -chain peptide is initiated by docking of the ligand peptide in the trench. A flexible extension of the N3 subdomain redirects towards N2, covers the trench-bound peptide and locks it

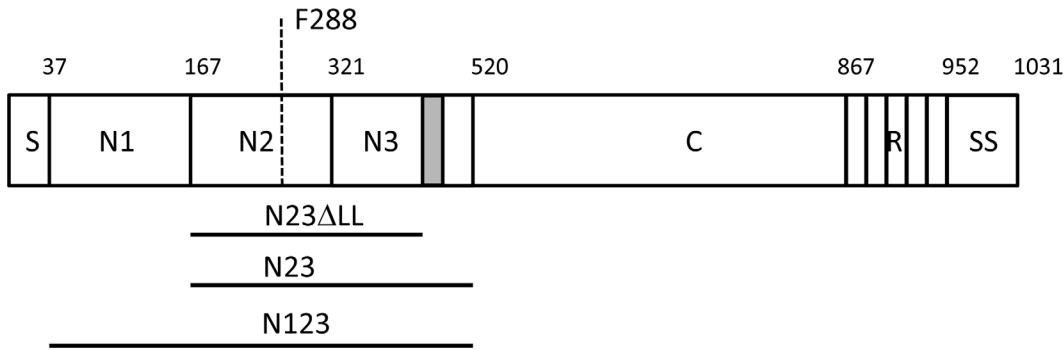


Figure 1. Schematic diagram of SpsD. The A domain modelled on the structure of ClfA spans residues 37–519 following the secretory signal sequence S. This is followed by a connecting region C (residues 521–867) and a repeat region R in strain ED99. The number of repeats varies from strain to strain resulting in proteins of slightly different sizes. A sorting signal (SS: LPXTG motif, hydrophobic domain and positively charged residues) occurs at the extreme C-terminus. The minimum ligand binding domain construct N2N3 spans residues 167–519. Residues comprising the ‘lock’ and ‘latch’ (grey box residues 490–499) are indicated (N23ΔLL). Residue F288 that is predicted to lie within the ligand binding trench is indicated by the dashed line.
doi:10.1371/journal.pone.0066901.g001

in place by β -strand complementation with a β sheet in subdomain N2. Structural and mechanistic studies strongly suggest that the N2N3 subdomains of FnBPA and FnBPB bind to the Fbg γ chain by the same mechanism. However differences exist in the repertoire of ligands bound in addition to Fbg, with ClfA recognizing complement factor I from human serum [19,20], FnBPA and FnBPB both additionally binding to elastin [17,21,22] and subdomains N2N3 of FnBPB also binding to fibronectin [23].

Clumping factor B is another MSCRAMM of *S. aureus* with an A domain that is similar in structure and function to ClfA but which binds different ligands to ClfA and FnBPs by the dock, lock and latch mechanism [24]. ClfB binds to the glycine and serine-rich omega loops that occur in the C-terminal tail of cytokeratin

10 and throughout the corneocyte envelope protein loricrin [25,26]. It also binds to a related sequence in the α C region of the α chain of Fbg [24,27].

Located distally to the A domains of FnBPA and FnBPB is an extended unfolded region comprising 11 or 10 tandemly repeated domains, respectively, that bind to the N-terminal type I modules of Fn by the tandem β -zipper mechanism [28,29]. In ClfA and ClfB this region is occupied by multiple repeats of the dipeptide Ser-Asp which have no known ligand binding function [30].

SpsD has been reported to promote bacterial adhesion to Fbg, K10 and Fn. In this study we set out to dissect SpsD and to localize and characterize its ligand binding region(s). We identified a region that is most closely related to the A domain of FnBPB of *S.*

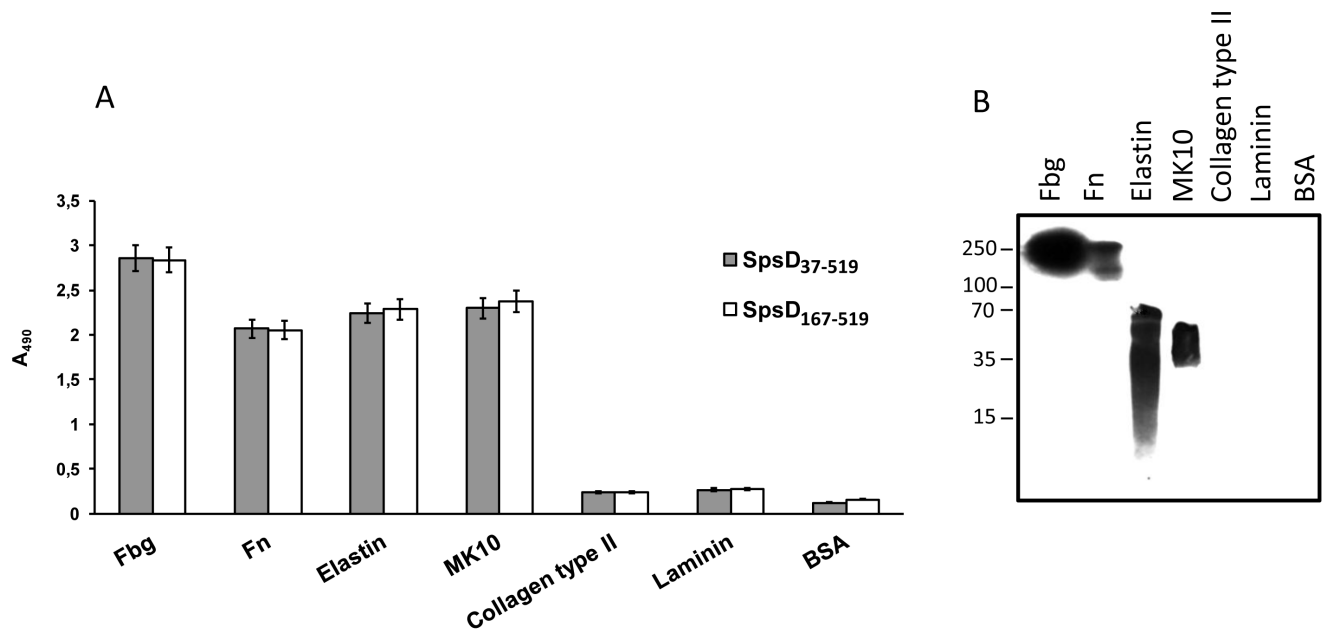


Figure 2. Binding of SpsD proteins to extracellular matrix or plasma proteins. (A), ligands were coated onto the surface of microtiter plates (1 μ g/well) and incubated with 17.5 nanomoles of SpsD₃₇₋₅₁₉ or SpsD₁₆₇₋₅₁₉, followed by mouse anti-His IgG and HRP-conjugated rabbit anti-mouse IgG. A, absorbance. (B), purified, unreduced human Fbg, Fn, α -elastin, mouse K10, collagen type II, laminin and BSA were subjected to SDS-PAGE, transferred to nitrocellulose filter and then incubated with SpsD₁₆₇₋₅₁₉, followed by incubation with mouse anti-SpsD₃₇₋₅₁₉ and HRP-conjugated rabbit anti-mouse antibodies. Molecular mass markers are indicated (kilodaltons).
doi:10.1371/journal.pone.0066901.g002

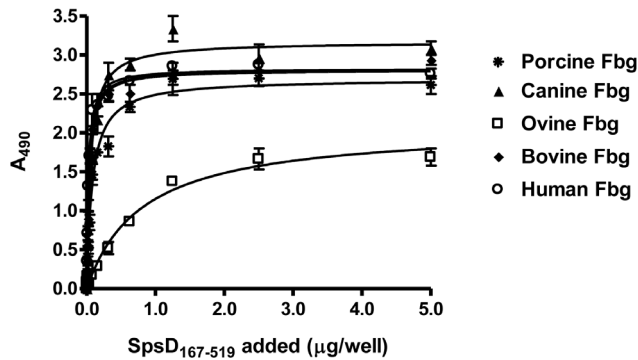


Figure 3. Dose-dependent binding of SpsD₁₆₇₋₅₁₉ to Fbg from different species. Microtiter wells were coated with human, canine, ovine, bovine and porcine Fbg overnight. The wells were probed with SpsD₁₆₇₋₅₁₉ followed by incubation with mouse anti-His-IgG and HRP-conjugated rabbit anti-mouse IgG. Values represent the means of triplicate samples \pm S.E. This experiment was performed three times with similar results.
doi:10.1371/journal.pone.0066901.g003

aureus that bound to these ligands and we provide insights into the ligand binding mechanism.

Materials and Methods

Bacterial Strains and Growth Conditions

Escherichia coli strain TOPP3 (Stratagene, La Jolla, CA, USA) was used as host for expression of recombinant proteins. *E. coli* strain TOPP3 was grown in Luria broth (LB) containing ampicillin (100 μ g/ml). *S. pseudintermedius* strain 326 was isolated from canine pyoderma [15]. Staphylococcal cells were grown for the indicated times at 37°C in BHI (Brain Heart Infusion) broth (BD, Sparks, MD, USA) with shaking.

Proteins

Fibronectin was purified from human plasma as previously reported [31]. The N-terminal fragment of Fn (N29) containing the five N-terminal type I modules, and the gelatin-binding domain (GBD) consisting of four type I modules and two type II modules were isolated following the protocol reported by Zardi *et al* [32]. The recombinant fragment corresponding to residues 607–1265 consisting of the first seven type III modules, the region including the amino acid residues 1266–1908 containing the extra domain B (EDB) plus type III modules 8–13 and the initial region of module 14, and C-terminal fragment 1913–2477 containing one type III module, the IIICS module, three type I modules and the site for interchain disulfide linkage of Fn were purchased from R&D Systems (Minneapolis, MN, USA). Human Fbg and α -elastin, a heterogeneous mixture of soluble peptides obtained from human lung, were obtained from Calbiochem (Merck, Darmstadt, Germany). Fbg was further purified on a gelatin-Sepharose column to remove contaminating Fn. The α -elastin preparation has a molecular weight of 10–60 kDa and runs as a smear on SDS-PAGE.

Bovine, porcine, ovine and canine Fbg as well as bovine serum albumin (BSA) were from Sigma (St Louis, MO, USA). Cultrex[®] murine sarcoma basement membrane laminin was purchased from Trevigen (Gaithersburg, MD, USA). The synthetic peptide corresponding to the C-terminus of the Fbg γ chain (residues 395–411) and the scrambled peptide were a generous gift by Dr I. Margarit (Novartis Diagnostics & Vaccines, Siena, Italy).

DNA Manipulation

DNA encoding the SpsD_{N1-N3} subdomains (SpsD₃₇₋₅₁₉), the SpsD_{N2-N3} region (SpsD₁₆₇₋₅₁₉) and SpsD_{N2-N3} lacking C-terminal residues (SpsD₁₆₇₋₄₉₈) were amplified by PCR using chromosomal DNA isolated from *S. pseudintermedius* 326 as template. All oligonucleotides were purchased from Integrated DNA Technologies (Leuven, Belgium). To amplify DNA encoding the N1–N3 domain, primer SpsD N1 forward (5'-GGCGGATCCGCTTCAGAAGT-3') and SpsD reverse (5'-GAGCTGCAGTAACTATATCC-3') were used. To amplify the N2–N3 region, the primers SpsD N2 forward (5'-GATGATCCGGAACAGATGT-3') and SpsD reverse were used. To amplify DNA encoding SpsD₁₆₇₋₄₉₈ the primers SpsD N2 forward and SpsD Δ LL reverse (5'-GTAGAAAGCAACCAT-TATCCC-3') were used. Restriction enzyme cleavage sites BamHI and PstI were incorporated at the 5' ends of the primers to facilitate cloning into the pQE30 expression plasmid (Qiagen, Chatsworth, CA, USA). Restriction enzymes were purchased from New England Biolabs (Hertfordshire, UK). The presence of appropriate DNA sequences was confirmed by sequencing (GATC Biotech, Konstanz, Germany). Amino-acid substitution F288A was introduced by site-directed mutagenesis using overlapping complementary primers (5'-CTTTATCTGGTTAATAGC-TAAGTTCAATGC and 5' GCATTGAACTTAGCTAT-TAAACCAGATAAAG-3'). The pQE30 plasmid containing DNA encoding amino acids SpsD₁₆₇₋₅₁₉ was used as template. Products were digested with DpnI to eliminate parental DNA and transformed into *E. coli*. The F228A amino-acid substitution was verified by DNA sequencing (Source Biosciences, Nottingham, UK).

Expression and Purification of Recombinant Proteins

Recombinant SpsD proteins were expressed from pQE30 plasmid in *E. coli* TOPP3. Overnight starter culture was diluted 1:50 in LB containing ampicillin (100 μ g/ml) and incubated with shaking until the culture reached A₆₀₀ 0.6–0.8. Recombinant protein expression was induced by addition of isopropyl 1-thio- β -D-galactopyranoside (0.1 mM) and continued for 4 h. Bacterial cells were harvested by centrifugation, and frozen at -80° C. Recombinant proteins were purified from cell lysates by Ni²⁺ affinity chromatography on a HiTrap chelating column (GE Healthcare). Protein purity was assessed by SDS-PAGE. Recombinant Bbp₂₇₀₋₅₉₉ [33], ClfA₄₀₋₅₅₉ [34], ClfB₂₀₁₋₅₄₂ [26], CNA₃₀₋₅₃₁ [35], FnBpB₁₆₃₋₄₈₀ [23] and SasG₅₀₋₄₂₈ [36] were each previously expressed with 6 x His N-terminal affinity tags using *E. coli* vectors and purified by Ni²⁺-chelate chromatography. Mouse cytokeratin 10 (residues 1–570, MK10₁₋₅₇₀), the N-terminal “head” domain (MK10₁₋₁₄₅) and the C-terminal “tail” region (MK10₄₅₄₋₅₇₀) proteins were prepared as reported previously [25]. GST fusion proteins containing the human Fbg γ -chain sequence (GST-Fbg γ ₃₉₅₋₄₁₁), human Fbg α -chain sequence (GST-Fbg α ₃₁₆₋₃₆₇) and the human K10 C-terminal “tail” region (GST-HK10₅₄₄₋₅₆₃) were described previously [26,37]. GST fusion proteins were purified on a GSTrap FF purification column (GE Healthcare) according to the manufacturer’s instructions.

SDS-PAGE and Western Blotting

SDS-PAGE was performed with a 10% polyacrylamide gel. The gels were stained with Coomassie Brilliant Blue (BioRad, Hercules, CA, USA). For the Western blot assay, human Fbg and Fn were subjected to SDS-PAGE and then electroblotted onto a nitrocellulose membrane (GE Healthcare). The membrane was treated with a solution containing 5% (w/v) dried milk in PBS, washed, and incubated with SpsD₁₆₇₋₅₁₉ (5 μ g/ml) for 1 h at 22°C.

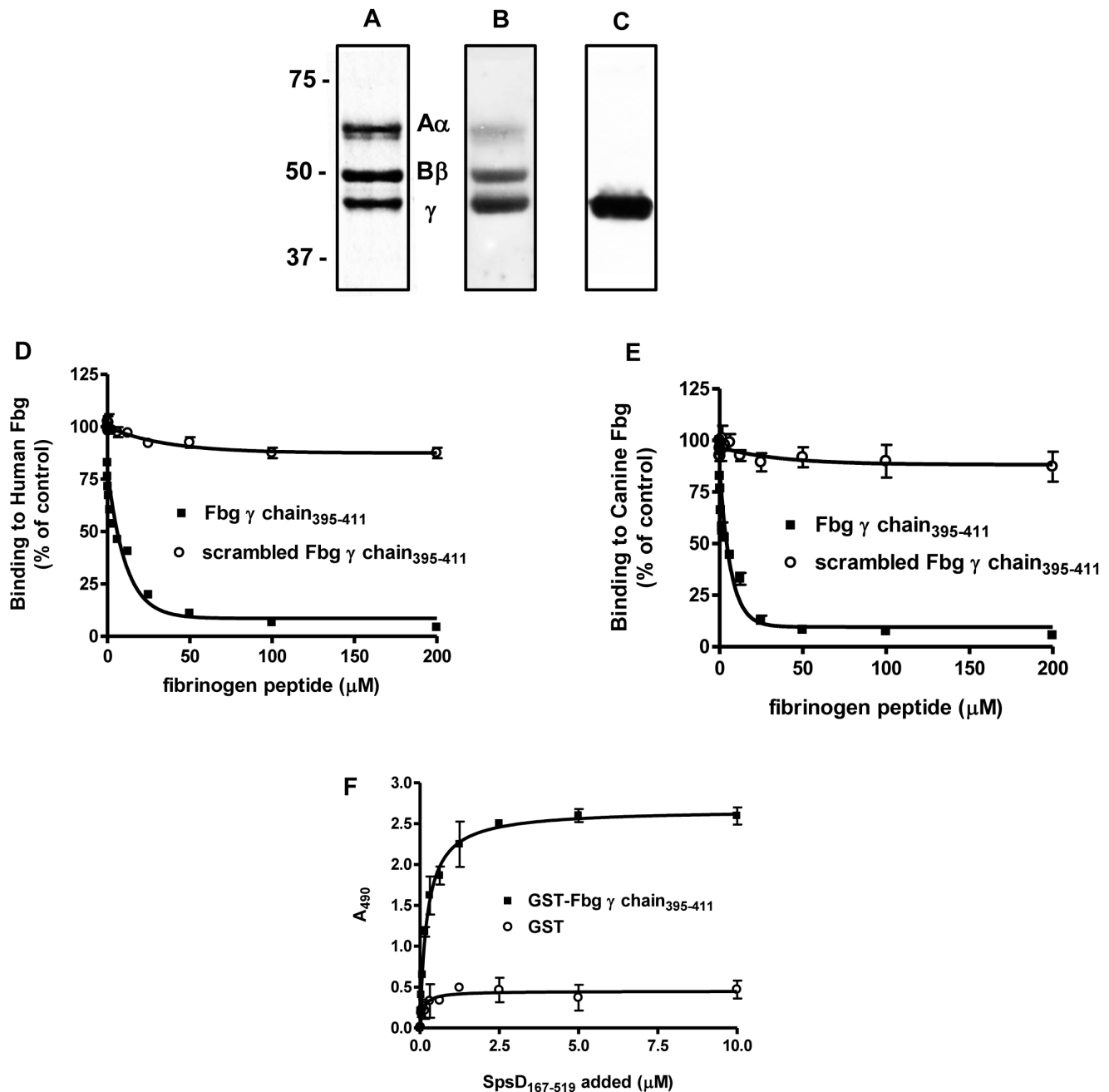


Figure 4. SpsD recognizes Fbg γ chain. (A), human Fbg was subjected to SDS-PAGE in reducing conditions and then stained with Coomassie Blue. (B), Fbg was subjected to SDS-PAGE in reducing conditions, transferred to a nitrocellulose membrane and Fbg chains detected by incubation of the membrane with anti-mouse Fbg IgG and then HRP-conjugated rabbit anti-mouse IgG. (C), Fbg was subjected to SDS-PAGE under reducing conditions, electroblotted onto nitrocellulose filter and probed with SpsD₁₆₇₋₅₁₉ followed by incubation with mouse anti-SpsD IgG and HRP-conjugated rabbit anti-mouse IgG. (D) and (E), effect of the Fbg C-terminal γ chain peptide on the binding of SpsD₁₆₇₋₅₁₉ protein to immobilized Fbg. Surface-coated human (D) or canine (E) Fbg was incubated with SpsD₁₆₇₋₅₁₉ in the presence of increasing concentrations of the 17-mer synthetic peptide of the γ chain. The effect of a scrambled peptide on Fbg-SpsD₁₆₇₋₅₁₉ interaction is also reported as control; the assay was performed as in (C). (F), dose-dependent binding of SpsD₁₆₇₋₅₁₉ protein to immobilized GST fused to the Fbg C-terminus of γ chain. Microtiter wells were coated with GST-Fbg γ chain and probed with increasing concentrations of SpsD₁₆₇₋₅₁₉. Complex formation was detected by addition of mouse anti-6-His IgG followed by HRP-conjugated rabbit anti-mouse IgG. Values are the means \pm S.E of triplicate wells and are representative of one experiment. This experiment was performed three times with similar results. doi:10.1371/journal.pone.0066901.g004

Following additional washings with 0.5% (v/v) Tween 20 in PBS (PBST), the membrane was incubated for 1 h with PBST containing an anti-His tag mouse monoclonal antibody (7E8) (2 $\mu\text{g}/\text{ml}$). After several washings in PBST, the membrane was

incubated for 45 min with HRP-conjugated rabbit anti-mouse IgG. Finally, the membrane was treated with ECL detection reagents 1 and 2 according to the procedure recommended by the

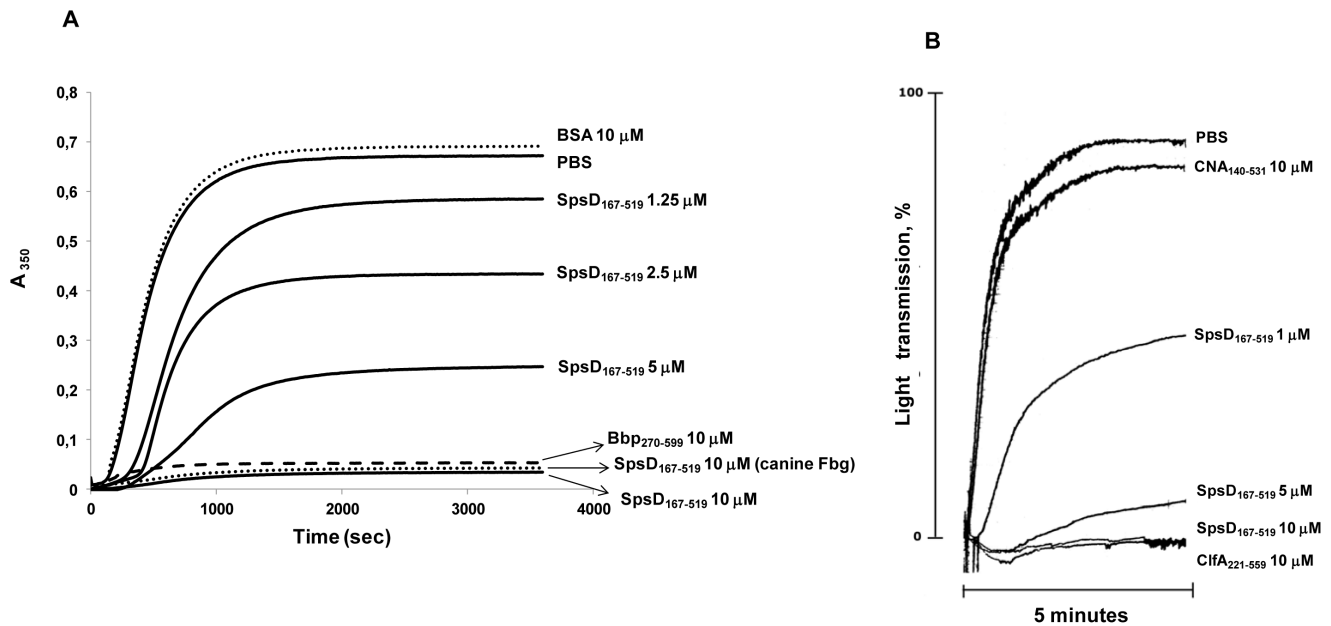


Figure 5. SpsD interferes with Fbg biological activities. (A), SpsD protein inhibits fibrin clot formation. Increasing amounts (1.25–10 μM) of SpsD₁₆₇₋₅₁₉ were preincubated with human Fbg prior to the addition of α-thrombin. Polymer formation was measured as a change in turbidity at 350 nm with time. The action of 10 μM Bbp₂₇₀₋₅₉₉ and BSA are shown as a positive and negative controls, respectively. The effect of 10 μM SpsD₁₆₇₋₅₁₉ on canine fibrin clot formation is also reported. (B), SpsD protein inhibits ADP-induced platelet aggregation. Washed human platelets (9×10^7) were preincubated in an aggregometer with the indicated concentrations of SpsD₁₆₇₋₅₁₉, ClfA₄₀₋₅₆₀ and CNA₃₀₋₅₃₁ in the presence of 200 μg/ml Fbg and 1 mM CaCl₂ at 37°C for 5 min and then added with 10 μM ADP. Platelet aggregation is expressed as the percentage of light transmission. The experiments have been repeated at least three times with similar results. doi:10.1371/journal.pone.0066901.g005

manufacturer (GE Healthcare) and exposed to an X-ray film for 30–60 s.

Antibodies

Mouse polyclonal antisera against SpsD₃₇₋₅₁₉, ClfB₄₄₋₅₄₂ and human Fbg were generated by injecting BALB/c mice intraperitoneally five times at 1-week intervals with 50 μg of the purified protein. The antigen was emulsified with an equal volume of complete Freund's adjuvant for the first immunization, followed by three injections in incomplete adjuvant. The mice were bled, and the sera were tested for reactivity to the purified antigen using ELISA and Western blot. The antibodies were purified by affinity chromatography on Protein A/G-Sepharose columns according to the recommendations of the manufacturer (GE Healthcare). Horseradish peroxidase (HRP)-conjugated rabbit anti-mouse antibody was from Dako (Glostrup, Denmark). 7E8 is an in-house generated monoclonal antibody recognizing recombinant His tagged proteins. This study was carried out in strict accordance with the recommendations in the Guide for the Care and Use of Laboratory Animals of the Italian Ministry of Health according to the European Union guidelines for the handling of laboratory animals. The protocol was approved by the local authorities ("Comitato Etico per la Sperimentazione Animale" of the University of Pavia, Italy) (Permit Number: 2–2012). The animals were sacrificed under lidocaine anesthesia, and all efforts were made to minimize suffering.

Binding of SpsD Proteins to Extracellular Matrix Proteins by Solid Phase Binding Assay

To screen binding of SpsD to extracellular matrix proteins, 1 μg of human Fbg, human Fn, human lung elastin, murine K10, bovine nasal septum type II collagen, murine sarcoma basement

membrane laminin and BSA were coated onto microtiter wells overnight at 4°C in 0.1 M carbonate buffer. The wells were washed, blocked with 2% BSA for 1 h at 22°C and incubated with SpsD₁₆₇₋₅₁₉ or SpsD₃₇₋₅₁₉ (17.5 nanomoles/well). Complex formation was detected with mouse anti-His tag antibody 7E8 (0.2 μg/well), followed by addition of peroxidase-conjugated rabbit anti-mouse IgG (1:1000) (Dako). Binding of SpsD₁₆₇₋₅₁₉ to Fbg from different species in ELISA format was performed by incubating 1 μg of the recombinant bacterial protein with each surface-coated Fbg type (1 μg/well) and detecting the bound protein as reported above.

Surface Plasmon Resonance (SPR)

All experiments were performed at 25°C on a BIAcore X instrument (Pharmacia Biosensor AB, Uppsala, Sweden). Purified human and canine Fbg, α-elastin or human Fn were covalently immobilized on the dextran matrix sensor chip surface (CM5 chip) by using a protein solution (30 μg/ml in 50 mM sodium acetate buffer, pH 5.5 for human and canine Fbg or 50 mM sodium acetate buffer, pH 4.0 for human Fn) in a 1:1 dilution with N-hydroxy-succinimide and N-ethyl-N'-3-(dimethylaminopropyl)-carbodiimide hydrochloride. The excess active groups on the dextran matrix were blocked with ethanolamine (1 M), pH 8.5 [38]. On another flow cell, the dextran matrix was treated as described above but without any ligand to provide an uncoated reference flow cell. The running buffer used was PBS containing 0.005% (v/v) Tween 20. Increasing concentrations of SpsD proteins were passed in succession over the ligand and reference surfaces without regeneration at the flow rate of 5 μl/min in running buffer.

To perform SPR experiments with GST-HK10₅₄₄₋₅₆₃, goat anti-GST antibody IgG (30 μg/ml) (GE Healthcare) was diluted in

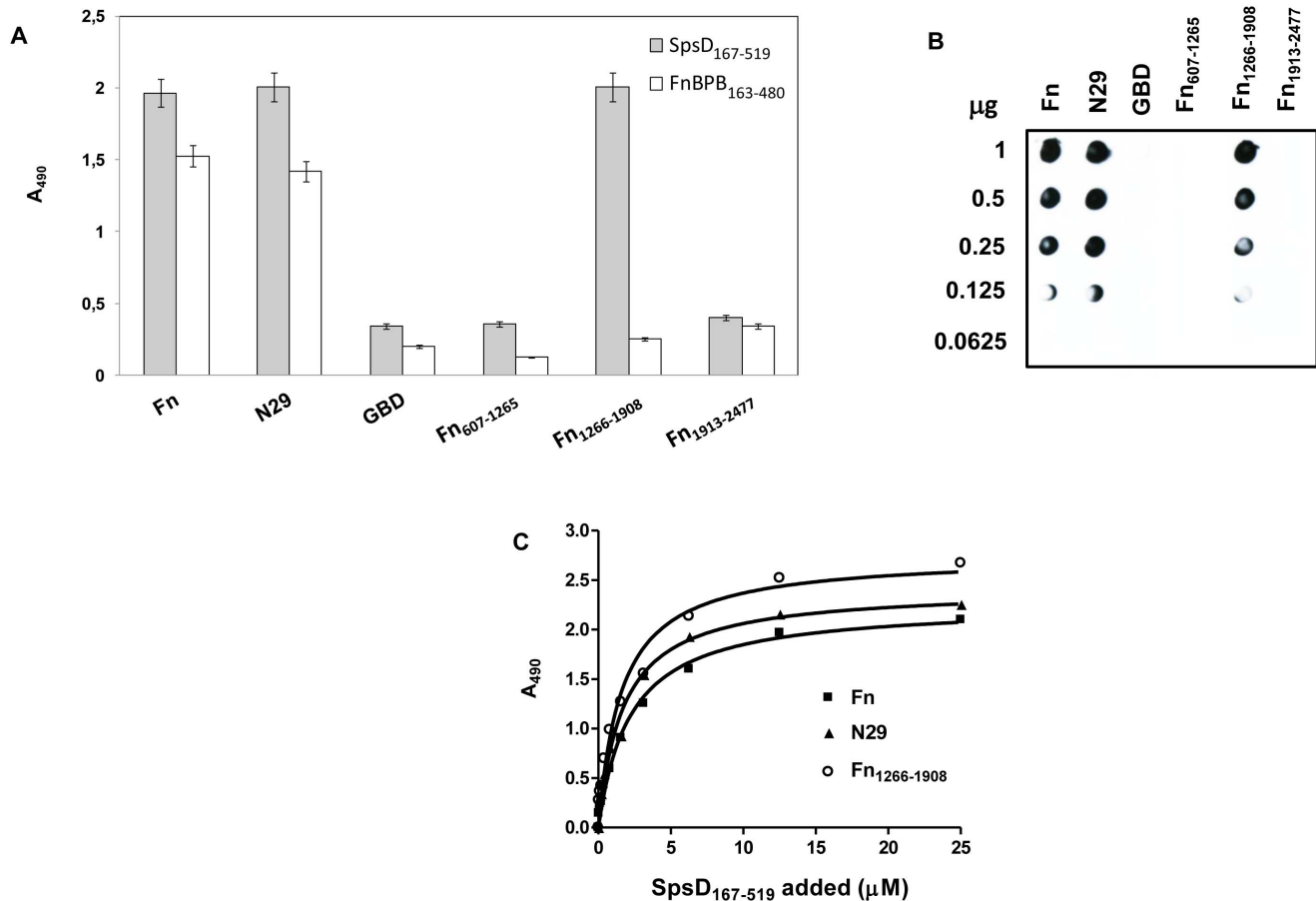


Figure 6. Localization of SpsD binding sites in Fn. (A), native Fn, the N29, the GBD, the recombinant fragments Fn₆₀₇₋₁₂₆₃, Fn₁₂₆₆₋₁₉₀₈ and the C-terminal region Fn₁₉₁₃₋₂₄₇₇ of Fn were immobilized onto a microtiter plate and then incubated with of SpsD₁₆₇₋₅₁₉. Bound protein was detected by addition to the wells of anti-SpsD₃₇₋₅₁₉ mouse antibody, followed by HRP-conjugated rabbit anti-mouse antibody. Binding of FnBPB₁₆₃₋₄₈₀ to Fn and its fragments reported as control was detected by addition to the wells of anti-FnBPB₁₆₃₋₄₈₀ rabbit IgG, followed by HRP-conjugated goat anti-rabbit antibody. (B), different amounts of Fn and Fn fragments (1000-62.5 ng) were dotted onto a nitrocellulose membrane, probed with SpsD₁₆₇₋₅₁₉ (1 μg/ml) and complexes detected by addition of mouse anti-SpsD₃₇₋₅₁₉ IgG, followed by HRP-conjugated rabbit anti-mouse IgG. (C), surface-coated Fn, the N29 fragment and the region including the aa residues 1266-1908 were incubated with increasing concentrations of SpsD₁₆₇₋₅₁₉ and complex formation detected as reported in (A). Results shown in panels A and C are the mean values of triplicate samples ± S.E. The experiments were repeated three times with similar results. doi:10.1371/journal.pone.0066901.g006

10 mM sodium acetate buffer, pH 5.0, and immobilized on carboxy-derivatized sensor chip. GST-HK10₅₄₄₋₅₆₃ (500 nM) was passed over a flow cell, while GST alone was passed over the other flow cell to provide a reference surface. Increasing concentrations of SpsD proteins were flowed over the surface of both flow cells without regeneration at a rate of 5 μl/min.

Sensorgrams from three sets of data for each of the protein concentrations were collected and averaged for each ligand. All of the sensorgram data presented were subtracted from the corresponding data from the reference flow cell. The data were analyzed using the BIAevaluation software version 3.0. A plot of the level of binding (response units) at equilibrium against concentration of ligand was used to determine the K_D .

Inhibition of the SpsD-Fbg Interaction

A solution of Fbg (10 μg/ml) was used to coat microtiter wells overnight at 4°C. The wells were washed three times with PBST and blocked with 2% (w/v) BSA in PBS for 1 h at 22°C. The wells were washed and 100 μl SpsD proteins (10 μg/ml) added after preincubation for 1 h at 22°C with a range of concentrations of a

synthetic peptide comprising the 17 C-terminal residues of the γ chain of Fbg or a scrambled peptide. The plates were incubated for 1 h at 22°C and bound protein detected by incubation with anti-His tag mouse 7E8 monoclonal antibody (0.2 μg/well) for 1 h at 22°C, followed by horseradish peroxidase-conjugated rabbit anti-mouse IgG serum. The percentage inhibition was calculated relative to the level of Fbg-bound protein detected in the absence of the inhibitor peptide.

Inhibition of Fibrin Clot Formation

Thrombin-catalyzed Fbg clotting was evaluated by incubating 150 μl of 3 μM Fbg in 20 mM Tris/HCl, pH 7.4 containing 200 mM NaCl and 5 mM CaCl₂ with the indicated concentrations of SpsD₁₆₇₋₅₁₉, Bbp₂₇₀₋₅₆₉ or BSA and 50 μl of thrombin (1.0 NIH unit/ml). Clot formation was measured as a change in turbidity with time related to the amount of the scattered light at 350 nm in a Jasco, V-630 spectrophotometer (Jasco, Tokyo, Japan).

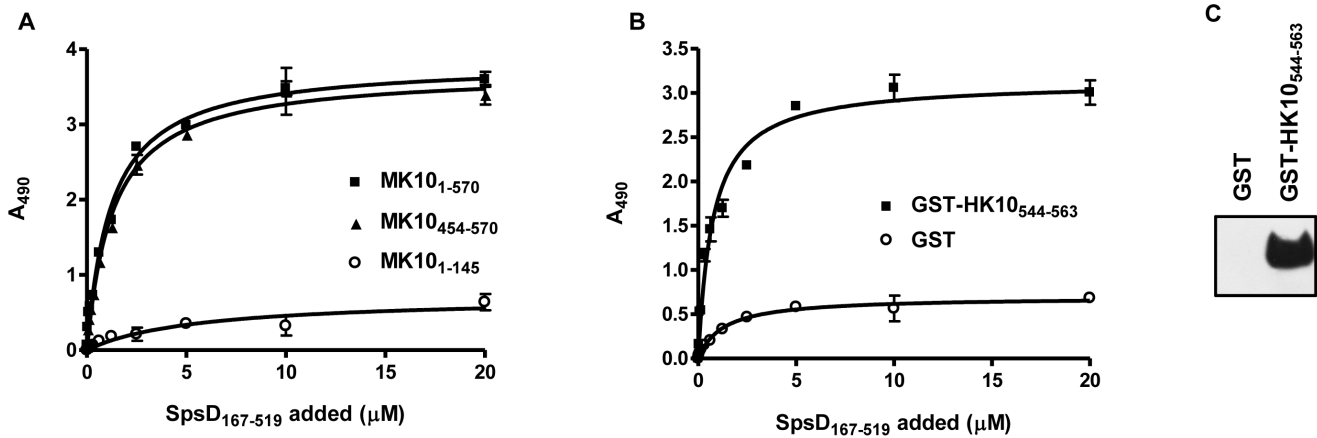


Figure 7. Binding of SpsD₁₆₇₋₅₁₉ to immobilized cytokeratin 10 proteins. (A), SpsD₁₆₇₋₅₁₉ was incubated in wells coated with recombinant mouse K10₁₋₅₇₀, K10₁₋₁₄₅ and K10₄₅₄₋₅₇₀. (B), SpsD₁₆₇₋₅₁₉ was added to ELISA wells coated with GST-human K10₅₄₄₋₅₆₃ (HK10₅₄₄₋₅₆₃); or GST alone. Bound SpsD₁₆₇₋₅₁₉ was detected by addition of mouse anti-SpsD₃₇₋₅₁₉ IgG, followed by HRP-conjugated rabbit anti-mouse IgG. (C), GST-HK10₅₄₄₋₅₆₃ or GST alone were subjected to SDS-PAGE, electroblotted onto nitrocellulose filter and probed with SpsD₁₆₇₋₅₁₉ followed by incubation with mouse anti-SpsD IgG and HRP-conjugated rabbit anti-mouse IgG. doi:10.1371/journal.pone.0066901.g007

Inhibition of Platelet Aggregation

300 µl (9 × 10⁷) washed platelets were preincubated in a Born aggregometer (Chrono-Log Havertown, PA, USA) with either buffer or the indicated concentrations of SpsD₁₆₇₋₅₁₉ or region A of ClfA or CNA in the presence of 200 µg/ml Fbg and 1 mM CaCl₂ at 37°C for 5 min. Then 10 µM ADP was added to trigger platelet activation and aggregation. The rate and extent of platelet aggregation was detected as the percentage of light transmission and presented as aggregation tracings.

SpsD Binding to Immobilized Fn Fragments by ELISA and Dot Blot

Fn fragments were used to identify binding sites of SpsD. Fn (1 µg/well) and Fn fragments (250 ng/well) were immobilized onto microtiter wells and then incubated with indicated concentrations of SpsD₁₆₇₋₅₁₉. Bound protein was detected using an anti-SpsD₃₇₋₅₁₉ mouse antibody followed by HRP-conjugated rabbit anti-mouse IgG. For dot blot experiments, different amounts of Fn and Fn fragments (1000- 62.5 ng) were dotted onto a nitrocellulose membrane, probed with SpsD₁₆₇₋₅₁₉ (1 µg/ml) and complexes detected as described above.

Results

Region A of SpsD

The sequence of the entire *spsD* gene of *S. pseudintermedius* ED99 is known. Here we describe the A domain of SpsD from strain 326 which was obtained following PCR amplification of genomic DNA. The A domains of SpsD from ED99 and 326 have the same number of residues and are 80% identical. They are most closely related to the A domain of FnBPB (40% and 42% identity to isoform I, respectively) [39] and they have 23% and 27% identity respectively to the A domain of ClfA from *S. aureus* Newman [40]. A 3D molecular model based on the crystal structure of ClfA allowed us to predict the coordinates of subdomains N1, N2 and N3 (Figure 1).

The SpsD A domain (N1N2N3 region) comprising residues 37–519 (SpsD₃₇₋₅₁₉) and the putative minimum ligand binding truncate comprising residues 167–519 (N2N3, SpsD₁₆₇₋₅₁₉) were cloned and expressed with 6 x His affinity tags.

Binding of Recombinant SpsD to Extracellular Matrix Proteins

Previous work has demonstrated that SpsD can promote bacterial adhesion to Fbg, Fn and K10 [11]. Here we sought to determine if the ligand binding ability resides in the N-terminal domain of the protein. An ELISA type ligand-binding assay was used to study the interaction of the recombinant SpsD proteins with surface-coated extracellular matrix proteins. SpsD₃₇₋₅₁₉ and SpsD₁₆₇₋₅₁₉ bound to immobilized Fbg, Fn and K10, as well as to α-elastin, while no interaction was observed with collagen, laminin or BSA (Figure 2A). The interaction of Fbg, Fn, K10 and α-elastin with the recombinant SpsD₁₆₇₋₅₁₉ protein was confirmed by Western ligand blotting where host proteins were electroblotted onto a nitrocellulose filter, probed with SpsD₁₆₇₋₅₁₉ and complex formation detected with a monoclonal antibody targeting the His-tag. Conversely, no interaction was observed when SpsD₁₆₇₋₅₁₉ was incubated with membrane-bound collagen type II, laminin or BSA (Figure 2B). Identical results were obtained with SpsD₃₇₋₅₁₉ (data not shown). Together these results suggest that the minimal region of SpsD required for binding to Fbg, Fn, K10 and elastin is the N2N3 subdomain. The absence of signal when Fbg, Fn, α-

Table 1. Summary of K_D ± SE values of SpsD proteins for extracellular matrix components.

	K _D (µM) ± SE	
	SpsD ₃₇₋₅₁₉	SpsD ₁₆₇₋₅₁₉
Human Fbg	0.380 ± 0.035	0.360 ± 0.032
Canine Fbg	0.367 ± 0.055	0.341 ± 0.056
Fn	2.350 ± 0.710	2.157 ± 0.702
α-Elastin	1.200 ± 0.220	1.020 ± 0.150
GST-HK10 ₅₄₄₋₅₆₃	0.906 ± 0.060	0.840 ± 0.032

doi:10.1371/journal.pone.0066901.t001

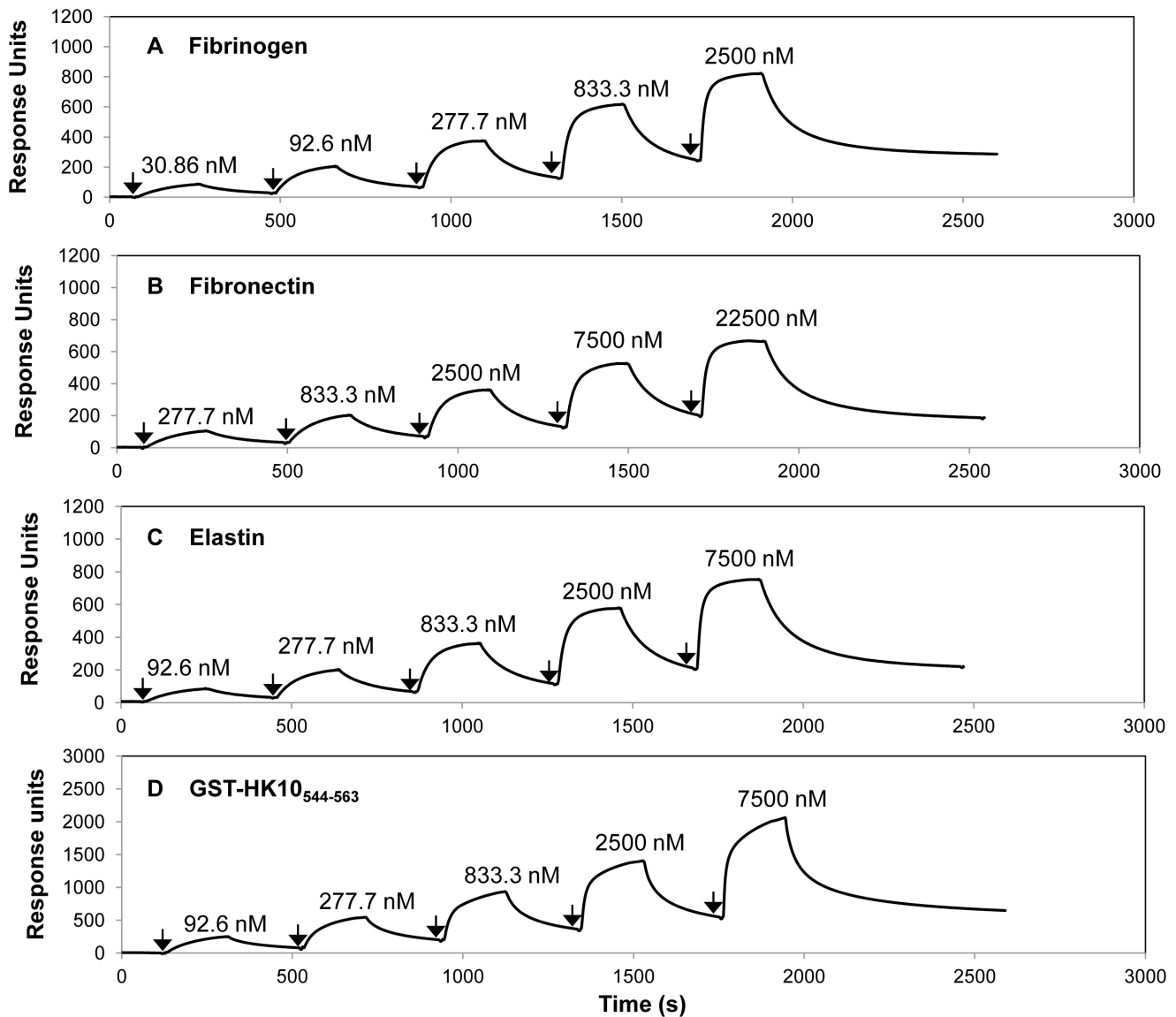


Figure 8. Surface Plasmon Resonance analysis of the interaction of SpsD₁₆₇₋₅₁₉ with Fbg, Fn, α -elastin and cytokeratin 10. Human Fbg (A), Fn (B) and α -elastin (C) were immobilized onto the surface of dextran chips. GST-human K10₅₄₄₋₅₆₃ (D) was captured onto a sensor chip coated with goat anti-GST IgG. Representative sensorgrams display binding of SpsD₁₆₇₋₅₁₉ to and dissociation from Fbg, Fn, α -elastin and GST-human K10₅₄₄₋₅₆₃, in a single cycle kinetics assay. Binding was measured as response units (RU) against time. The affinities were calculated from curve fitting to a plot of the RU values against concentrations of SpsD. Arrows indicate the time at which SpsD₁₆₇₋₅₁₉ was injected. The data shown is representative of 3 individual experiments.

doi:10.1371/journal.pone.0066901.g008

elastin and K10 were tested for binding to His-tagged *S. aureus* MSCRAMM SasG₅₀₋₄₂₈ either in ELISA or Western blotting, further demonstrates the specificity of SpsD₁₆₇₋₅₁₉ interaction with host ligands (data not shown).

Next we determined the ability of SpsD₁₆₇₋₅₁₉ protein to recognize Fbg molecules obtained from different animals. Increasing amounts of SpsD₁₆₇₋₅₁₉ were added to surface-coated human, porcine, canine, bovine and ovine Fbg and the binding was measured. SpsD₁₆₇₋₅₁₉ bound to each of the different types of Fbg with similar affinities with exception of the ovine protein (Figure 3).

SpsD Binds the C-terminus of the γ -chain of Fbg

Western ligand blotting was employed to determine if SpsD bound to the α -, β - or γ - chain of Fbg. Human Fbg was reduced with dithiothreitol and the three chains separated by SDS-PAGE (Figure 4A). Efficient transfer to a control nitrocellulose membrane was shown by probing with anti-Fbg IgG (Figure 4B). Another membrane was incubated with recombinant His-tagged SpsD₁₆₇₋₅₁₉ and when probed with a monoclonal antibody recognizing the His-tag only the γ -chain reacted (Figure 4C).

ClfA, FnBPA and FnBPB are known to bind to a short sequence at the extreme C-terminus of the γ -chain of Fbg while ClfB binds to repeat number 5 of the α chain. To determine if SpsD bound the same γ chain residues as ClfA, the ability of a 17 residue synthetic peptide comprising the C-terminal residues of the Fbg γ -

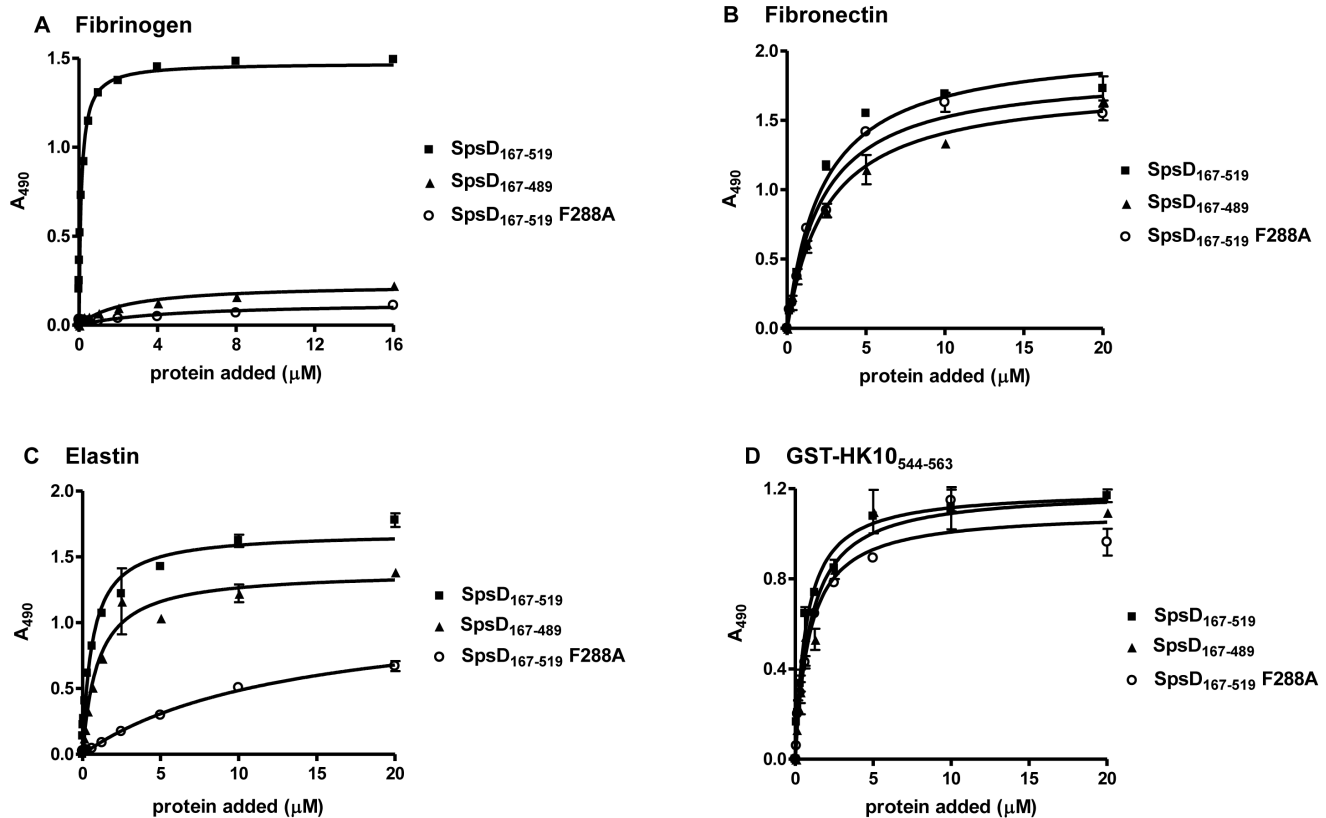


Figure 9. Binding of SpsD₁₆₇₋₅₁₉, SpsD₁₆₇₋₅₁₉ F288A and SpsD₁₆₇₋₅₁₉ latch mutant to immobilized Fbg, Fn, α -elastin and K10. Microtiter wells were coated with human Fbg (A), Fn (B), α -elastin (C) and K10 (D) in a bicarbonate buffer overnight. The wells were probed with increasing concentrations of SpsD proteins followed by incubation with mouse anti SpsD₃₇₋₅₁₉ IgG and HRP-conjugated rabbit anti-mouse IgG. Values are the means \pm S.E of triplicate wells and are representative of one experiment. This experiment was performed three times with similar results.

doi:10.1371/journal.pone.0066901.g009

chain to inhibit binding of SpsD₁₆₇₋₅₁₉ to immobilized Fbg was tested. The peptide strongly inhibited the binding of SpsD to human and canine Fbg dose-dependently while a scrambled peptide had no effect (Figure 4D and 4E).

Finally, direct binding of SpsD to the Fbg γ -chain peptide coupled to GST that had been immobilized on the surface of an ELISA plate was tested. As shown in Figure 4F, SpsD bound dose-dependently and saturably to GST-Fbg $\gamma_{395-411}$ with a half maximum binding concentration of $0.32 \pm 0.02 \mu\text{M}$ but not at all to the GST control. Thus, SpsD binds to the same C-terminal Fbg γ -chain residues as ClfA and the FnBPs.

Region A of SpsD Interferes with Fibrin Clot Formation and Platelet Aggregation

Several adhesins not only interact with the target molecule in the host but also neutralize and even disrupt the biological function of the target. For example, ClfA, although it does not interfere with catalytic activity of thrombin, by binding to the C-terminus of γ chain it affects fibrin clot formation by abrogating fibrin monomer polymerization and cross-linking of Fbg γ chains [41]. Therefore, we examined the effect of SpsD on fibrin clot formation. Human Fbg was preincubated with different concentrations (1.25–10 μM) of SpsD₁₆₇₋₅₁₉ prior to the addition of thrombin. In these conditions SpsD inhibited coagulation as effectively as Bbp₂₇₀₋₅₉₉, a recently identified Fbg-binding protein from *S. aureus* [33] (Figure 5A). Conversely, no effect was observed when Fbg was preincubated with 10 μM BSA. Consistent with the

indication that SpsD recognizes the C-terminus of the γ chain of canine Fbg, we also observed that preincubation of canine Fbg with 10 μM SpsD resulted in complete inhibition of clot formation.

It is well known that the C-terminus of Fbg γ chain contains the platelet integrin GPIIb/IIIa recognition sequence (QAGDV⁴¹¹) [42] and that a monoclonal antibody that recognizes the γ chain C-terminus of Fbg exerts inhibitory effects on platelet aggregation [43]. Thus, SpsD was tested for its impact on ADP-induced platelet aggregation. As depicted in Figure 5B, ADP-stimulated platelet aggregation was inhibited in a dose-dependent manner by SpsD. In contrast, the collagen-binding domain of the *S. aureus* adhesin CNA (CNA₃₀₋₅₃₁), did not affect the process. Together these data demonstrate that SpsD could act as a modulator of thrombus formation.

Binding Sites in Fibronectin for SpsD

To locate the binding site(s) in Fn for the A domain of SpsD, the binding of SpsD₁₆₇₋₅₁₉ to the Fn N29 domain, the gelatin binding domain and the segments spanning residues 607–1265, 1266–1908 and 1913–2477 was tested. Native Fn and the purified fragments were immobilized onto microtiter wells, probed with SpsD₁₆₇₋₅₁₉ and complex formation detected with anti-SpsD IgG. A strong signal was observed when SpsD₁₆₇₋₅₁₉ was incubated with full length Fn, the N29 fragment and the segment spanning the residues 1266–1908 (Fn₁₂₆₆₋₁₉₀₈), while the other fragments failed to bind (Figure 6A). A similar assay was performed with

FnBPB_{163–480} and confirmed its ability to bind to full length Fn and the N29 fragment and not to the C-terminal Fn_{1266–1908} fragment [23]. The binding of SpsD to the two different regions of Fn was confirmed by incubating the Fn fragments with SpsD_{167–519} in a dot blot assay (Figure 6B). Finally, as shown in Figure 6C, binding of SpsD_{167–519} to both the N29 and the Fn_{1266–1908} fragment was concentration-dependent and saturable. The affinity for each domain appeared to be similar with half maximum binding concentrations of $2.21 \pm 0.30 \mu\text{M}$ for N-terminal domain and $1.97 \pm 0.3 \mu\text{M}$ for Fn_{1266–1908}.

SpsD Binds to the K10 Tail Region

ClfB binds to the C-terminal tail region of K10 [25]. To determine if SpsD binds to the same domain, recombinant proteins comprising full length murine K10 along with the N-terminal head and C-terminal tail regions, were immobilized into microtitre wells and tested for their ability to support SpsD binding. SpsD_{167–519} bound to full length K10 and the tail region dose-dependently and saturably and with half maximal binding concentrations of 1.02 ± 0.25 and $1.2 \pm 0.1 \mu\text{M}$, respectively (Figure 7A).

ClfB is known to bind to glycine (G)-serine (S)-rich domains within the omega loop regions in the C-terminal tail of K10, in loricrin and in the α -chain of Fbg [26]. To determine if SpsD could bind to the same sequences, recombinant SpsD_{167–519} was tested in solid phase binding assays with GST-HK10_{544–563}. The SpsD protein bound dose-dependently and saturably but failed to bind to the GST (Figure 7B). This interaction was confirmed by Western blot (Figure 7C). However, in contrast to ClfB, SpsD did not interact with Fbg α chain (Figure S1). Consistent with this, GST-Fbg α _{316–367} inhibited binding of ClfB, but not that of SpsD_{167–519}, while GST-Fbg γ _{395–411} blocked the interaction of SpsD_{167–519} but not that of ClfB with Fbg (Figure S2). Thus SpsD bound the same GS-rich omega loop in K10 as ClfB but surprisingly failed to recognize the Fbg α chain.

Measurements of Dissociation Constants of SpsD for Host Ligands by Surface Plasmon Resonance

Binding of SpsD_{167–519} to human Fbg, Fn, α -elastin or GST-HK10_{544–563} immobilized on a sensor chip was analyzed by SPR using BIAcore X. Increasing concentrations of SpsD_{167–519} were passed over the surface of each ligand-coated chip: in these conditions SpsD_{167–519} bound to the ligand in a dose dependent manner. From analysis of the equilibrium binding data, the dissociation constant (K_D) for the interaction between SpsD_{167–519} and Fbg was determined to be $0.360 \pm 0.032 \mu\text{M}$ (Figure 8A and Table 1). SpsD_{167–519} showed a dissociation constant value for canine Fbg comparable to that reported for human Fbg (Table 1).

SpsD_{167–519} bound Fn with a K_D of $2.16 \pm 0.70 \mu\text{M}$, indicating that the affinity of the recombinant SpsD protein for Fn was lower than that exhibited for Fbg (Figure 8B and Table 1). The K_D values of SpsD_{167–519} for α -elastin and GST-HK10_{544–563} were 1.02 ± 0.15 and $0.84 \pm 0.032 \mu\text{M}$, respectively (Figure 8, panels C and D and Table 1). Very similar K_D values were obtained when SpsD_{37–519} was passed over sensor chips coated with these proteins (Table 1).

Ligand Binding by SpsD_{167–519} Mutants

One goal of this work was to determine whether the N2N3 subdomains of SpsD bind Fbg by the same mechanism as the A domains of ClfA and FnBPs. Our previous work demonstrated that the C-terminal residues of the N3 subdomain of FnBPB were crucial for its interaction with Fbg [23]. As SpsD interacts with the

Fbg γ -chain with a high affinity, it was proposed that the C-terminal 20 residues of the N3 subdomain of SpsD form the locking and latching segment and play a similar role in the interaction of SpsD with Fbg. To test this, a recombinant truncate of the SpsD_{167–519} protein, which lacked the predicted locking and latching segment (SpsD_{167–498}: Δ LL, Figure 1), was expressed and its ability to bind to immobilized Fbg was analysed by ELISA. No detectable interaction was observed when increasing concentrations of SpsD_{167–499} were incubated with Fbg-coated microtitre wells (Figure 9A), while a small but remarkable reduction in elastin binding was noticed (Figure 9C). In contrast, no reduction in binding was observed when increasing amounts of SpsD_{167–499} were incubated with surface-coated Fn or K10 (Figure, 9 panels B and D). To investigate further if SpsD binds to the ligands at same or different sites, an amino acid substitution was introduced in SpsD_{167–519} at residue F288. F288 is predicted to be located within the ligand binding trench and is in an equivalent position to the crucial residues F314 of FnBPB and Y338 of ClfA. SpsD F288A binding to Fbg and elastin was greatly reduced showing that F288 is indeed important for ligand binding and supports the notion that both Fbg and elastin bind to the same or overlapping regions of SpsD. Conversely, a small reduction was observed when SpsD F288A was tested for binding to Fn or K10.

Discussion

The ability of *S. aureus* cells to adhere to components of the extracellular matrix is promoted by several distinct surface proteins called MSCRAMMs. The mechanistic basis of many of the interactions has been very well characterized by structural analysis and by probing function with appropriate variant mutant proteins. By molecular modelling and mutagenesis it is possible to infer/predict that proteins with similar structural organization bind their ligands by the same mechanism as those that have been investigated in detail.

The A domain of ClfA is the archetype of a family of proteins that fold into three subdomains called N1, N2 and N3, the last two of which are the absolute minimum required for ligand binding by the “dock, latch and lock (DLL)” mechanism [18]. The A domain of ClfA binds to the γ -chain of Fbg by DLL and it does not interact with Fn, elastin or K10 [44–46]. In contrast, the A domain of ClfB binds by DLL to the α -chain of Fbg and also to K10. In both cases the DLL mechanism was shown by X-ray crystal structure and supported by the loss of binding by mutants that had substitutions in the ligand binding trench (trench mutants) or which lack the C-terminal lock-latch domain (LL mutants) [24].

The Fn binding proteins FnBPA and FnBPB are composed of two distinct ligand binding domains. Their A domains are most closely related to ClfA and bind to the Fbg γ -chain [16,23]. In contrast to ClfA, both FnBPA and FnBPB also bind to elastin [21] and in the case of FnBPB, Fn [23]. Binding to Fbg and elastin most likely occurs by DLL as indicated by studies with mutant proteins [17]. Ten or 11 tandemly repeated domains at the C-termini of FnBPA and FnBPB bind to Fn with high affinity by the tandem β zipper mechanism [29].

The SpsD protein of *S. pseudintermedius* was previously shown to promote bacterial adhesion to Fbg, Fn and K10 [11,15]. In this study we have dissected the SpsD protein and have investigated how a single protein can bind to such a disparate array of ligands. Bioinformatic analysis predicted that the N-terminal region folded into a typical A domain composed of subdomains N1 N2 and N3 and was most closely related in sequence identity to FnBPB [11]. Although there is a repeat domain at the C-terminus of SpsD, the

individual repeats are shorter than, and bear no similarity to, the Fn-binding repeats of FnBPs [11].

The recombinant A domain of SpsD was shown here to bind to the γ -chain of Fbg (and not to the α -chain), to K10, to Fn and also to elastin. There are intriguing similarities to and differences from the MSCRAMM A domains of *S. aureus*.

To investigate if the DLL mechanism is involved in ligand binding, Δ LL and trench mutants of the N2N3 construct were expressed and purified. Binding to Fbg γ -chain was completely abrogated in the SpsD Δ LL and trench mutants indicating that binding to this ligand occurred by DLL. However SpsD also bound to K10 which is a defining property of ClfB, while ClfB binds to the α -chain and not to the γ -chain of Fbg [27]. The ligand peptide sequences that bind to the trench are completely dissimilar. Indeed structural biology showed that the Fbg α -chain peptide and the K10 omega loop peptide bound to the same part of the ligand binding trench of ClfB and a consensus motif was identified [24]. Therefore it was intriguing to discover that the Δ LL and trench mutants of SpsD bound to K10 with the same affinity as the wild-type while similar mutants of ClfB were previously shown to be defective in binding to both ligands [24]. We can only conclude that SpsD binding to K10 does not occur by DLL and propose a distinct K10 binding site in N2N3.

Like its closest relative FnBPB, SpsD also binds to elastin. This most likely occurs by DLL because the trench and the Δ LL mutants were both defective in binding to this ligand. Although a similar investigation was not carried out with FnBPB, detailed studies with the A domain of FnBPA supported the DLL mechanism for elastin binding [17]. This confirms the close relationship of the A domain of SpsD to those of the FnBPs.

It was not clear if the binding of FnBPB A domain to Fn occurred by DLL because the Δ LL truncate bound Fn with the same affinity as the wild-type while a trench mutant was defective in both Fbg and Fn binding. It seemed that the Fn binds to FnBPB in the trench region but that lock latch aspect of DLL is not involved [23]. The SpsD A domain shares with FnBPB the ability to bind Fn but with the difference that it bound to two distinct domains within the host protein while FnBPB only recognized the N29 fragment [23]. This might explain why both the SpsD Δ LL and trench mutants bound Fn while the Δ LL mutant of FnBPB was defective.

A domains can be stitched onto distinct “stalks” (B repeats, Sdr repeats, Fn-binding repeats, or to a complete different sequence in SpsD). The DLL binding mechanism in N2N3 regions has evolved to binds to different ligands. Indeed even the orientation of a peptide ligand can vary [24]. Many have acquired the capacity to bind ligands by mechanisms other than DLL although the binding

of a large folded ligand might occlude the trench region and block DLL mechanism of binding to other ligands.

In conclusion, SpsD appears to be the most promiscuous staphylococcal adhesin so far identified and possibly is a factor involved in *S. pseudintermedius* colonization of the host. In future studies the three-dimensional structure of the apo-protein and ligand bound SpsD may provide molecular details on these multiple interactions and give additional insights to better understand the role played by this microorganism in human and animal pathogenesis.

Supporting Information

Figure S1 Binding of SpsD_{167–519} or ClfB_{201–542} to Fbg and Fbg α chain. Increasing concentrations of SpsD_{167–519} (A) or ClfB_{201–542} (B) were incubated in wells coated with 500 ng/well human Fbg, GST in fusion with the α chain peptide (aa 316–367) or GST alone. Bound ligand was detected by addition of mouse anti-SpsD_{37–519} IgG or anti-ClfB_{45–542} IgG followed by HRP-conjugated rabbit anti-mouse IgG. Results shown in the panels are the mean values of triplicate samples \pm S.E. The experiments were repeated three times with similar results. (TIF)

Figure S2 Effect of Fbg recombinant chains on the binding of SpsD_{167–519} or ClfB_{201–542} to surface-coated Fbg. 500 ng SpsD_{167–519} (A) or ClfB_{201–542} (B) mixed with increasing amounts of GST-tagged α chain, GST in fusion with the C-terminus of the γ chain, or GST alone were added to and incubated with microtiter wells coated with Fbg (500 ng/well). Bound ligand was detected by addition of mouse anti-SpsD_{37–519} IgG or anti-ClfB_{45–542} IgG followed by HRP-conjugated rabbit anti-mouse IgG. Results shown in the panels are the mean values of triplicate samples. Error bars show the standard deviation. The experiments were repeated three times with similar results. (TIF)

Acknowledgments

The authors are grateful to Dr. Sofia Giorgetti and Prof. G. Merlini for assistance and advice with BIAcore measurements and Dr. Lina Cipolla for performing platelet aggregation experiments.

Author Contributions

Conceived and designed the experiments: GP JAG TJF PS. Performed the experiments: GP JAG SR ADP AM VC. Analyzed the data: GP JAG TF PS. Contributed reagents/materials/analysis tools: GP JAG TJF PS. Wrote the paper: GP JAG TJF PS.

References

- Perreten V, Kadlec K, Schwarz S, Grönlund Andersson U, Finn M, et al. (2010) Clonal spread of methicillin-resistant *Staphylococcus pseudintermedius* in Europe and North America: an international multicentre study. *J Antimicrob Chemother* 65: 1145–1154.
- Weese J, van Duijkeren E (2010) Methicillin-resistant *Staphylococcus aureus* and *Staphylococcus pseudintermedius* in veterinary medicine. *Vet Microbiol* 140: 418–429.
- Stegmann R, Burnens A, Maranta CA, Perreten V (2010) Human infection associated with methicillin-resistant *Staphylococcus pseudintermedius* ST71. *J Antimicrob Chemother* 65: 2047–2048.
- Gerstadt K, Daly JS, Mitchell M, Wessolossky M, Cheeseman SH (1999) Methicillin-resistant *Staphylococcus intermedius* pneumonia following coronary artery bypass grafting. *Clin Infect Dis* 29: 218–219.
- Kempker R, Mangalat D, Kongphet-Tran T, Eaton M (2009) Beware of the pet dog: a case of *Staphylococcus intermedius* infection. *Am J Med Sci* 338: 425–427.
- Campanile F, Bongiorno D, Borbone S, Venditti M, Giannella M (2007) Characterization of a variant of the SCCmec element in a bloodstream isolate of *Staphylococcus intermedius*. *Microb Drug Resist* 13: 7–10.
- Onuma K, Tanabe T, Sato H (2012) Antimicrobial resistance of *Staphylococcus pseudintermedius* isolates from healthy dogs and dogs affected with pyoderma in Japan. *Vet Dermatol* 23: 17–22.
- Laarhoven LM, de Heus P, van Luijn J, Duim B, Wagenaar JA, et al. (2011) Longitudinal study on methicillin-resistant *Staphylococcus pseudintermedius* in households. *Plos One* 6: e27788.
- Tse H, Tsoi HW, Leung SP, Urquhart IJ, Lau SK, et al. (2011) Complete genome sequence of the veterinary pathogen *Staphylococcus pseudintermedius* strain HKU10–03, isolated in a case of canine pyoderma. *J Bacteriol* 193: 1783–1784.
- Ben Zakour NL, Bannoehr J, van den Broek AH, Thoday KL, Fitzgerald JR (2011) Complete genome sequence of the canine pathogen *Staphylococcus pseudintermedius*. *J Bacteriol* 193: 2363–2364.
- Bannoehr J, Ben Zakour NL, Reglinski M, Inglis NF, Prabhakaran S, et al. (2011) Genomic and surface proteomic analysis of the canine pathogen *Staphylococcus pseudintermedius* reveals proteins that mediate adherence to the extracellular matrix. *Infect Immun* 79: 3074–3086.
- McEwan NA (2000) Adherence by *Staphylococcus intermedius* to canine keratinocytes in atopic dermatitis. *Res Vet Sci* 68: 279–283.

13. McEwan NA, Kalna G, Mellor D (2005) A comparison of adherence by four strains of *Staphylococcus intermedius* and *Staphylococcus hominis* to canine corneocytes collected from normal dogs and dogs suffering from atopic dermatitis. *Res Vet Sci* 78: 193–198.
14. Bannoehr J, Brown JK, Shaw DJ, Fitzgerald RJ, van den Broek AH, et al. (2012) *Staphylococcus pseudintermedius* surface proteins SpsD and SpsO mediate adherence to ex vivo canine corneocytes. *Vet Dermatol* 23: 119–124.
15. Geoghegan JA, Smith EJ, Speziale P, Foster TJ (2009) *Staphylococcus pseudintermedius* expresses surface proteins that closely resemble those from *Staphylococcus aureus*. *Vet Microbiol* 138: 345–352.
16. Wann ER, Gurusiddappa S, Höök M (2000) The fibronectin-binding MSCRAMM FnbpA of *Staphylococcus aureus* is a bifunctional protein that also binds to fibrinogen. *J Biol Chem* 275: 13863–13871.
17. Keane FM, Loughman A, Valtulina V, Brennan M, Speziale P, et al. (2007) Fibrinogen and elastin bind to the same region within the A domain of fibronectin binding protein A, an MSCRAMM of *Staphylococcus aureus*. *Mol Microbiol* 63: 711–723.
18. Ponnuraj K, Bowden MG, Davis S, Gurusiddappa S, Moore D, et al. (2003) A “dock, lock, and latch” structural model for a staphylococcal adhesin binding to fibrinogen. *Cell* 115: 217–228.
19. Hair PS, Ward MD, Semmes OJ, Foster TJ, Cunnion KM (2008) *Staphylococcus aureus* clumping factor A binds to complement regulator factor I and increases factor I cleavage of C3b. *J Infect Dis* 198: 125–133.
20. Hair PS, Echague CG, Sholl AM, Watkins JA, Geoghegan JA, et al. (2010) Clumping factor A interaction with complement factor I increases C3b cleavage on the bacterial surface of *Staphylococcus aureus* and decreases complement-mediated phagocytosis. *Infect Immun* 78: 1717–1727.
21. Roche FM, Downer R, Keane F, Speziale P, Park PW, et al. (2004) The N-terminal A domain of fibronectin-binding proteins A and B promotes adhesion of *Staphylococcus aureus* to elastin. *J Biol Chem* 279: 38433–38440.
22. Keane FM, Clarke AW, Foster TJ, Weiss AS (2007) The N-terminal A domain of *Staphylococcus aureus* fibronectin-binding protein A binds to tropoelastin. *Biochemistry* 46: 7226–7232.
23. Burke FM, Di Poto A, Speziale P, Foster TJ (2011) The A domain of fibronectin-binding protein B of *Staphylococcus aureus* contains a novel fibronectin binding site. *FEBS J* 278: 2359–2371.
24. Ganesh VK, Barbu EM, Deivanayagam CC, Le B, Anderson AS, et al. (2011) Structural and biochemical characterization of *Staphylococcus aureus* clumping factor B/ligand interactions. *J Biol Chem* 286: 25963–25972.
25. Walsh EJ, O'Brien LM, Liang X, Höök M, Foster TJ (2004) Clumping factor B, a fibrinogen-binding MSCRAMM (microbial surface components recognizing adhesive matrix molecules) adhesin of *Staphylococcus aureus*, also binds to the tail region of type I cytokeratin 10. *J Biol Chem* 279: 50691–50699.
26. Mulcahy ME, Geoghegan JA, Monk IR, O'Keefe KM, Walsh EJ, et al. (2012) Nasal Colonisation by *Staphylococcus aureus* Depends upon Clumping Factor B Binding to the Squamous Epithelial Cell Envelope Protein Loricrin. *Plos Pathog* 8: e1003092.
27. Walsh EJ, Mijajlovic H, Gorkun OV, Foster TJ (2008) Identification of the *Staphylococcus aureus* MSCRAMM clumping factor B (ClfB) binding site in the alphaC-domain of human fibrinogen. *Microbiology* 154: 550–558.
28. Schwarz-Linek U, Werner JM, Pickford AR, Gurusiddappa S, Kim JH, et al. (2003) Pathogenic bacteria attach to human fibronectin through a tandem beta-zipper. *Nature* 423: 177–181.
29. Meenan NA, Visai L, Valtulina V, Schwarz-Linek U, Norris NC, et al. (2007) The tandem beta-zipper model defines high affinity fibronectin-binding repeats within *Staphylococcus aureus* FnbpA. *J Biol Chem* 282: 25893–25902.
30. Hartford O, Francois P, Vaudaux P, Foster TJ (1997) The dipeptide repeat region of the fibrinogen-binding protein (clumping factor) is required for functional expression of the fibrinogen-binding domain on the *Staphylococcus aureus* cell surface. *Mol Microbiol* 25: 1065–1076.
31. Speziale P, Visai L, Rindi S, Di Poto A (2008) Purification of human plasma fibronectin using immobilized gelatin and Arg affinity chromatography. *Nat Protoc* 3: 525–533.
32. Zardi L, Carnemolla B, Balza E, Borsi L, Castellani P, et al. (1985) Elution of fibronectin proteolytic fragments from a hydroxyapatite chromatography column. A simple procedure for the purification of fibronectin domains. *Eur J Biochem* 146: 571–579.
33. Vazquez V, Liang X, Horndahl JK, Ganesh VK, Smeds E, et al. (2011) Fibrinogen is a ligand for the *Staphylococcus aureus* microbial surface components recognizing adhesive matrix molecules (MSCRAMM) bone sialoprotein-binding protein (Bbp). *J Biol Chem* 286: 29797–29805.
34. O'Connell DP, Nanavaty T, McDevitt D, Gurusiddappa S, Höök M, et al. (1998) The fibrinogen-binding MSCRAMM (clumping factor) of *Staphylococcus aureus* has a Ca²⁺-dependent inhibitory site. *J Biol Chem* 273: 6821–6829.
35. Rich RL, Deivanayagam CC, Owens RT, Carson M, Höök A, et al. (1999) Trench-shaped binding sites promote multiple classes of interactions between collagen and the adherence receptors, alpha(1)beta(1) integrin and *Staphylococcus aureus* cna MSCRAMM. *J Biol Chem* 274: 24906–24913.
36. Roche FM, Massey R, Peacock SJ, Day N, Visai L, et al. (2003) Characterization of novel LPXTG-containing proteins of *Staphylococcus aureus* identified from genome sequences. *Microbiology* 149: 643–654.
37. Geoghegan JA, Ganesh VK, Smeds E, Liang X, Höök M, et al. (2010) Molecular characterization of the interaction of staphylococcal microbial surface components recognizing adhesive matrix molecules (MSCRAMM) ClfA and Fbl with fibrinogen. *J Biol Chem* 285: 6208–6216.
38. Johnsson B, Löfås S, Lindquist G (1991) Immobilization of proteins to a carboxymethyl-dextran-modified gold surface for biospecific interaction analysis in surface plasmon resonance sensors. *Anal Biochem* 198: 268–277.
39. Burke FM, McCormack N, Rindi S, Speziale P, Foster TJ. (2010) Fibronectin-binding protein B variation in *Staphylococcus aureus*. *BMC Microbiol* 10: 160. doi: 10.1186/1471-2180-10-160.
40. McDevitt D, Francois P, Vaudaux P, Foster TJ. (1995) Identification of the ligand-binding domain of the surface-located fibrinogen receptor (clumping factor) of *Staphylococcus aureus*. *Mol Microbiol* 16: 895–907.
41. Liu CZ, Shih MH, Tsai PJ (2005) ClfA(221–550), a fibrinogen-binding segment of *Staphylococcus aureus* clumping factor A, disrupts fibrinogen function. *Thromb Haemost* 94: 286–294.
42. Kloczewiak M, Timmons S, Hawiger J (1983) Recognition site for the platelet receptor is present on the 15-residue carboxy-terminal fragment of the gamma chain of human fibrinogen and is not involved in the fibrin polymerization reaction. *Thromb Res* 29: 249–255.
43. Jirousková M, Smyth SS, Kudryk B, Coller BS (2001) A hamster antibody to the mouse fibrinogen gamma chain inhibits platelet-fibrinogen interactions and FXIIIa-mediated fibrin cross-linking, and facilitates thrombolysis. *Thromb Haemost* 86: 1047–1056.
44. Hawiger J, Kloczewiak M, Bednarek MA, Timmons S (1989) Platelet receptor recognition domains on the alpha chain of human fibrinogen: structure-function analysis. *Biochemistry* 28: 2909–2914.
45. McDevitt D, Nanavaty T, House-Pompeo K, Bell E, Turner N, et al. (1997) Characterization of the interaction between the *Staphylococcus aureus* clumping factor (ClfA) and fibrinogen. *Eur J Biochem* 247: 416–424.
46. Ganesh VK, Rivera JJ, Smeds E, Ko YP, Bowden MG, et al. (2008) A structural model of the *Staphylococcus aureus* ClfA-fibrinogen interaction opens new avenues for the design of anti-staphylococcal therapeutics. *PLoS Pathog* 4: e1000226.